Journal of Magnetics 11(3), 130-134 (2006)

RF Characterizations of Patterned CoNbZr Magnetic Thin Film on Transmission Line

Ki Hyeon Kim*

Department of Physics, Yeungnam University, Gyeongsan 712-749, Korea

(Received 18 August 2006)

The microwave power absorption for the patterned CoNbZr magnetic film has been investigated by coplanar waveguide method. The power absorption peaks of the patterned CoNbZr film (50 μm × 2 mm × 2 μm), were observed at around 5.7 GHz. The observed resonance peak was in good agreement with calculated ferromagnetic resonance frequency including magnetic shape anisotropy effects. Compared with the coplanar waveguide without a magnetic film, the characteristic impedance of patterned film was shown to be increased. This resulted from the large increment of inductance up to 33 % without any significant changes of the capacitance.

Key words : ferromagnetic resonance, patterned magnetic film, coplanar waveguide, propagation constant, noise suppression, wavelength shortening, scattering parameter, relative permeability

1. Introduction

As increasing the switching frequency in electronic devices and components, the magnetic thin films have been required to operate at high frequency with controllable switching loss. These magnetic thin films have been widely used for the electromagnetic high frequency devices such as radio frequency (RF) noise suppressor, thin film inductor, phase shifter, and tunable filters up to a few GHz frequencies [1-3]. In these devices, the change of the characteristic impedance should be minimized to avoid signal distortion in a broadband frequency region from MHz up to GHz range. More detailed mechanism of the countermeasure for the electromagnetic noise emission and radio frequency (RF) thin inductor by the integrated magnetic films on signal transmission line was briefly explained elsewhere [1, 4]. To evaluate the switching frequency of the integrated magnetic thin films, the transmission line like a micro strip line and coplanar waveguide (CPW) are widely used for broadband GHz frequency switching circuit as a representative signal transmission line.

To make the structure and geometry of the microwave power absorption system using transmission line, it is critical to characterize the characteristic impedance (Z_c) of the integrated magnetic film on signal transmission line for applications of electromagnetic devices like magnetic thin inductor, filter, electromagnetic noise countermeasure etc.. Basically, CPW shows the broad pass-band frequency characteristics up to a few tenth of GHz without any significant change of characteristic impedance.

Therefore, we systematically investigated the frequency swept microwave absorption and characteristic impedance changes of integrated CoNbZr magnetic films using a broadband CPW and a network analyzer.

2. Experimental Procedure

The CPW with 50 Ω-characteristic impedance was fabricated on the 7059 corning glass (permittivity, $\varepsilon_r = 5.84$) substrate, which is calculated using Muller and Hilberg equations [5]. As shown in Fig. 1 a), an integrated device is composed of magnetic film (2000 μm × 50 μm × 2 μm ($l \times w \times t$))/2 μm-thick polyimide/Cu transmission line (2200 μm × 50 μm × 3 μm($l \times w \times t$))/ seed layer (Cu/Ti)/ glass substrate, which was fabricated by a photolithography process. The Cu/Ti seed layers were deposited by rf sputtering to the thickness of 1000 Å and 100 Å, respectively. Fig. 1 b) shows the top view of fabricated CPW. The 3 μm-thick Cu transmission lines were deposited by Cu electroplating method whose electrolyte was composed of $CuSO_4$, H_2SO_4 and deionized (DI) water.

The polyimide as an insulator between CPW and magnetic film was spin-coated and cured at 400 °C in N_2 atmosphere. Amorphous $Co_{85}Nb_{12}Zr_3$ magnetic films were

*Corresponding author: Tel: +82-53-810-2334,
Fax: +82-53-810-4616, e-mail: kee1@ynu.ac.kr

deposited by RF magnetron sputtering on polyimide layer /CPW as shown in Fig. 1 c). And then the magnetic film was patterned by photolithography and etched by ion milling. The polyimide on contact pad was etched by reactive ion etching (RIE) using mixed CF_4 and Ar gas. In order to control the uniaxial magnetic anisotropy field (H_k) and align the direction of spins on magnetic film, the magnetic film was annealed at about 300 °C during 1 hour with ~3 kG of the external magnetic field. The saturation magnetization ($4\pi M_s$) of theses films is about 10 kG and in-plane magnetic anisotropy field (H_k) about 10 Oe. The intrinsic FMR frequency of CoNbZr film exhibits about 0.9 GHz without the consideration about magnetic shape anisotropy. The easy axes of CoNbZr magnetic film integrated on CPW were aligned in parallel to the wave propagation ($\mathbf{h}_{rf}$) of the CPW.

The electric performance is measured with two Ground-Signal-Ground pins type wafer probes mechanically touched at the left and right most ends of the transmission line from 0.1 GHz to 20 GHz using HP 8720D network analyzer.

3. Results and Discussions

To evaluate the microwave power absorption and change of characteristic impedance (Z_c), the scattering parameters (S_{11}, S_{21}) of CPW were measured by network analyzer.

Fig. 1 a) shows the patterned magentic film on transmission line for S-parameter charterization. A piece of interconnect with charcteristic impedance, Z_c and propagation constant, γ is placed in an S-parameter test system of impedance Z_0=50 Ω. The resulting S-parpmeter matrix is determined by the incident power a_1 and a_2 and the reflected power b_1 and b_2 [6].

The transmission parameters wirh the change of frequency have been extracted directly from S-parameter measurement data. Once these transmission parameters are determined, small signal frequency domain response is known and the large time-domain response can be obtained by inverse Fourier transform due to the linearity of the response with voltage. Signal transmisson is based on the solution of the classical Telegrapher's transmission line equation. The S-papameter responses measured from a lossy unmatched transmission line length (l) with g and Z_c in a Z_0 impedance system are [6-8]

$$[S]=\frac{1}{D_s}\begin{bmatrix}(Z_c^2-Z_0^2)\sinh\gamma l & 2Z_cZ_0\\ 2Z_cZ_0 & (Z_c^2-Z_0^2)\sinh\gamma l\end{bmatrix} \quad (1)$$

Where, $D_s=2(Z_cZ_0)\cos\gamma l(Z_c^2+Z_0^2)\sinh\gamma l$

Since the above matrix is symmetrical, it contains two

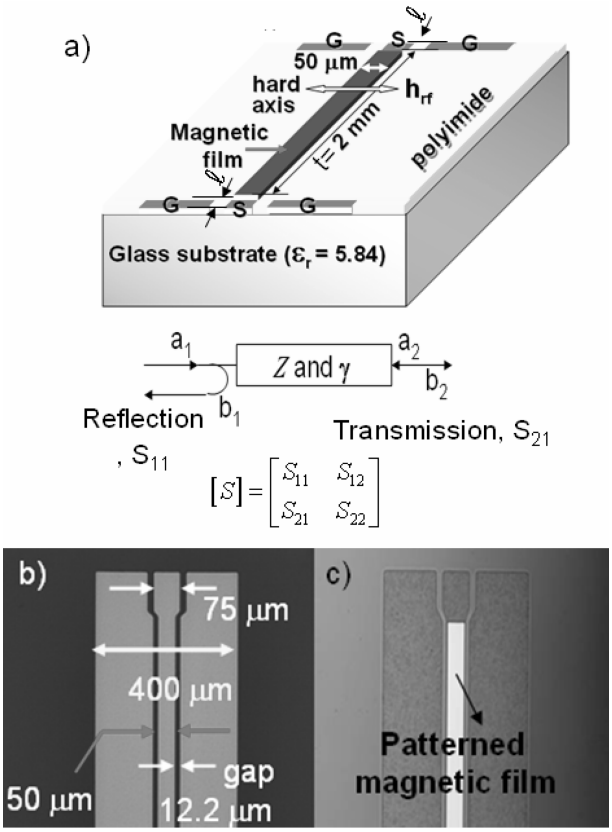

Fig. 1. Schematic of the integrated magnetic film on coplanar waveguide a) and top view of the optical microscope image of coplanar waveguide b) and patterned magnetic film c).

independent linear equations. This S-parameter matrix is converted to ABCD parameters which incorporate the interconnect propagation constant $\gamma(\omega)$ and impedance $Z(\omega)$ more explicitly. The equivalent ABCD matrix is

$$[ABCD]=\begin{bmatrix}\cosh\gamma l & Z_c\sinh\gamma l\\ \frac{\sinh\gamma l}{Z_c} & \cosh\gamma l\end{bmatrix} \quad (2)$$

The relationship between the S-parameter and ABCD matrix is [6-8]

$$\begin{aligned}A &= (1+S_{11}-S_{22}-\Delta S)/(2S_{21})\\ B &= (1+S_{11}+S_{22}+\Delta S)Z_0/(2S_{21})\\ C &= (1-S_{11}-S_{22}+\Delta S)/(2S_{21}Z_0)\\ D &= (1-S_{11}+S_{22}-\Delta S)/(2S_{21})\end{aligned} \quad (3)$$

Where $\Delta S=S_{11}S_{22}-S_{21}S_{22}$

Equation (1)-(3) are combined to yield:

$$e^{-\gamma l}=\left\{\frac{1-S_{11}^2+S_{21}^2}{2S_{21}}\pm K\right\}^{-1} \quad (4)$$

Where,

$$K=\left\{\frac{(S_{11}^2-S_{21}^2+1)^2-(2S_{11})}{(2S_{21})^2}\right\}^{1/2} \quad (5)$$

$$Z_c^2=Z_0^2\frac{(1+S_{11})^2-S_{21}^2}{(1-S_{11})-S_{21}^2} \quad (6)$$

During the extraction of complex parameters γ and Z from $e^{-\gamma l}$ and Z_c^2, the cyclically mapped phase output of S-parameter network analyzer (–180° to +180°) is converted value.

Once γ and Z are determined, then from standard transmission line relationships:

$$\gamma=\sqrt{(R+j\omega L)(G+j\omega C)}=\alpha+j\beta \quad (7)$$

$$Z=\sqrt{\frac{(R+j\omega L)}{(G+j\omega C)}} \quad (8)$$

Then $R=\mathrm{Re}\{\gamma Z_c\},\ L=\mathrm{Im}\{\gamma Z_c\}/\omega,$
$G=\mathrm{Re}\{\gamma/Z_c\},\ C=\mathrm{Im}\{\gamma Z_c\}/\omega$

Fig. 2 shows the transmission (S_{21}) and reflection (S_{11}) signal of the CPW and CoNbZr on CPW, respectively. The transmission signal (S_{21}) of CPW is gradually attenuated a little with the increase of frequency. When the magnetic film is integrated on CPW, transmission signal shows the big attenuation at specific frequency about 5.7 GHz. It implies that the transmission power through CPW is absorbed in magnetic film. This power absorption can be analyzed by the change of characteristic impedance with the change of inductance and capacitance.

Fig. 3 a) shows the inductance and the capacitance of the integrated magnetic film on CPW in comparison with that of CPW without any load. The inductance is increased by magnetic film, while the capacitances do not show

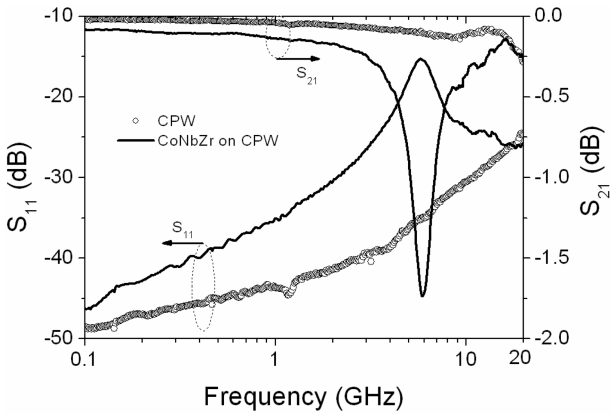

Fig. 2. The measured s-parameter (S_{21}, S_{11}) of CPW and CoNbZr on CPW.

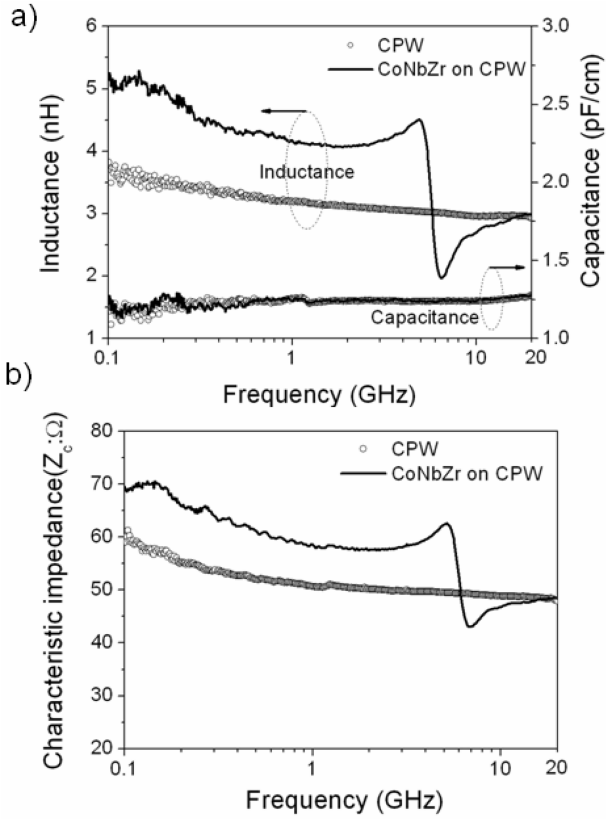

Fig. 3. The change of the inductance, capacitance a) and characteristic impedance b) of CoNbZr magnetic film and CPW with increment of the frequency.

any large variation in comparison with that of CPW. As a result, the characteristic impedance of magnetic film is increased to 8 Ω at 1 GHz in comparison with that of CPW, as shown in Fig. 3 b). These variations of characteristic impedance arise from the change of inductance and resistance of the magnetic film.

The resonance frequency of the power absorption was observed at around 5.7 GHz which resonance frequency was shifted to high frequency in comparison with that of CoNbZr film without shape anisotropy [9].

The formula for the resonance condition with the consideration of demagnetization condition is given by [10-12]

$$f_r=\frac{\gamma}{2\pi}\sqrt{(H_k+(N_y-N_z)2\pi M_s)(H_k+(N_x-N_z)4\pi M_s)} \quad (9)$$

Where, f_r, γ, H_k, and $4\pi M_s$ denote, respectively, resonance frequency, gyromagnetic ratio, magnetic anisotropy field, and the saturation magnetization. The demagnetizing factors N_x, N_y, and N_z are determined by the dimension of the magnetic film [11].

In general, we can express unknown relative permeability, $\mu_r=\mu_r'-j\mu_r''$ using transmission line method. When

transmission line is loaded with sample material, the characteristic impedance (Z_c) can be expressed, where [6]

$$Z_C = Z_0\sqrt{\frac{\mu_r}{\varepsilon_r}} \tag{10}$$

In unloaded regions, the propagation constant in free space is $\gamma_0 = \omega\sqrt{\mu_0\varepsilon_0}$, while in the loaded region, propagation constant is generally complex and is designated by γ, where

$$\gamma = \gamma_0\sqrt{\mu_r\varepsilon_r} \tag{11}$$

At the plane boundaries between unloaded and loaded at both side, there are complex reflection coefficients R and –R, respectively, where

$$R = \frac{Z_c - Z_0}{Z_c + Z_0} \tag{12}$$

Using (10), equations (11) and (12) may be solved simultaneously to yield the desired parameters [12]

$$\mu_r = \frac{\gamma}{\gamma_0}\left(\frac{1+R}{1-R}\right) \tag{13}$$

Thus, knowing γ and R enables μ_r to be calculated. The values may be found from the values of S_{11} and S_{21} which measured at the input and output terminals in Fig. 1 a).

Finally, we can extract the S-parameter using [T] matrix as follows

$$S_{21} = S_{12} = \frac{(1-R^2)e^{-j2\gamma_0 l}}{e^{j\gamma t} - R^2 e^{-j\gamma t}} \tag{14}$$

$$S_{11} = S_{22} = \frac{j2Re^{-j2\gamma_0 l}\sin\gamma t}{e^{j\gamma t} - R^2 e^{-j\gamma t}} \tag{15}$$

Equations (14) and (15) may now be solved simultaneously for γt and R in terms of the known and measured quantities [6, 13].

$$\gamma t = \cos^{-1}\left(\frac{e^{-j4\gamma_0 l} + S_{21}^2 - S_{11}^2}{2e^{j2\gamma_0 l}S_{21}}\right) = \cos^{-1}(\arg) \tag{16}$$

$$R = S_{11}/(e^{-j2\gamma_0 l} - S_{12}e^{-j\gamma l}) \tag{17}$$

And μ_r can be obtained through (16) and (17).

Fig. 3 shows the calculated permeability frequency profile by Landau-Lifshitz-Gilbert equation [12] in comparison with that of equation (13) using the measured data. The calculated resonance frequency was coincidence with the measured ferromagnetic resonance frequency by CPW cell.

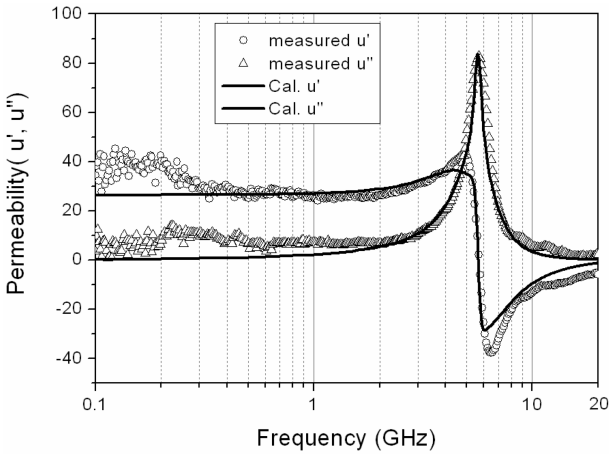

Fig. 4. The measured permeability frequency profile of CoNbZr magnetic film in comparison with that of the calculated by LLG equation.

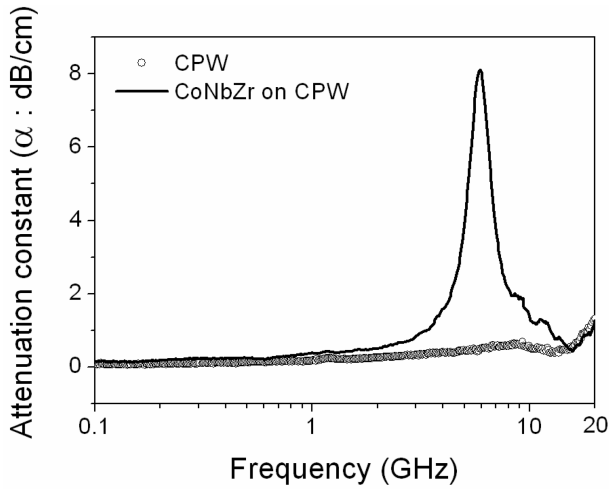

Fig. 5. The attenuation constant of the CoNbZr magnetic film on CPW in comparison with that of CPW without magnetic film.

Fig. 5 shows the signal attenuation of the CoNbZr magnetic film on CPW in comparison with that of CPW. Maximum attenuation is generated about 8 dB/cm at broad-band frequency about 3 GHz to 10 GHz. It implies that controllable attenuation can be used for electromagnetic noise suppressor by absorption power and also for the microwave band-stop filter.

In general, the phase variation of propagation signal should be minimized to enhance the signal integrity in electronic devices. However, the phase variation of propagation signal due to the insertion of magnetic film shortens the propagation wavelength over a broad frequency range.

The propagation wavelength (γ) is given $\gamma = \alpha + j\beta$, where, γ is propagation constant, α is attenuation constant, and β is phase ($= 2\pi/\lambda$). In Fig. 6, the propagation

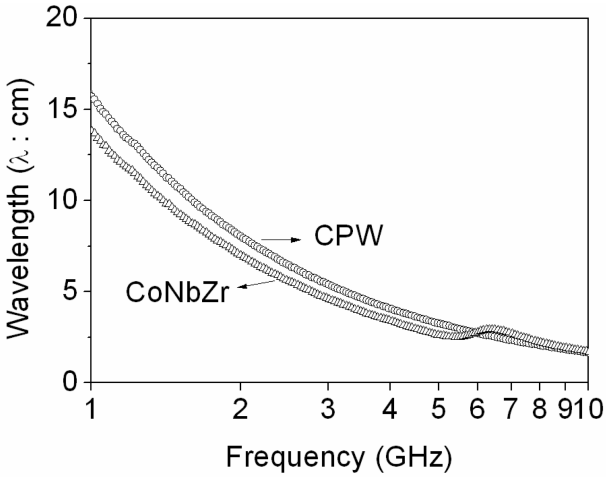

Fig. 6. The propagation wavelength shortening by integration of magnetic film on CPW.

wavelengths are obtained with increment of frequency. The propagation wavelength by patterned magnetic film exhibits about 13.82 cm at 1 GHz, which are about 10~15% shorter than that of the CPW (15.68 cm) without magnetic film. It implies that wavelength shortening by magnetic film is expected to promise the size reduction of electronic devices.

4. Coclusions

The characteristic impedance was slightly increased up to10 W in comparison with that of CPW. It implies that the characteristic impedance can be controlled by properties and shape of the magnetic film. As results, the integrated magnetic film on CPW shows a good potential for near field electromagnetic noise countermeasure and RF & microwave filters. The signal cut-off frequency can be controlled up to a few GHz by the controlling magnetic anisotropy of the magnetic film without any external applied magnetic fields. In addition, with insertion of the magnetic film on signal transmission line, the propagation wavelengths shorten about 15 % in comparison with that of CPW.

Acknowledgement

This research was supported by the Yeungnam University research grants in 2006. The author would like to thank to Prof. Masahiro Yamaguchi in Tohoku University for fruitful discussion and help with experimental facilities.

References

[1] Ki Hyeon Kim, Masahiro Yamaguchi, Phys. Stat. Sol.(b) **241**(7), 1761 (2004).
[2 Bijoy Kuanr, L. Malkinski, R. E. Camley, and Z. Celinski, P. Kabos, J. Appl. Phys. **93**(10), 8591 (2003).
[3] A. L. Adenot, O. Acher, T. Taffary, P. Queffelec, and G. Tanne, J. Appl. Phys. **87**(9), 6914 (2000).
[4] S. Yoshida, H. Ono, S. Ando, F. Tsuda, T. Ito, Y. Shimada, M. Yamaguchi, K.I. Arai, S. Ohnuma, T. Masumoto, IEEE Trans. Magn. **37**, 2401 (2001).
[5] B. C. Wadell, Transmission Line Design Handbook, Norwood, MA: Artech House, (1991).
[6] David M. Pozar, Microwave Engineering, John Wiley & Sons, Inc. (1998).
[7] William R.Eisenstadt, Yungseon Eo, IEEE Trans. Comp. and Manufact. Techn. **15**(4), 483 (1992).
[8] K. C. Gupta, R. Grag, and R. Chada, Computer aided Design of Microwave Circuits, Dedham, MA: Artech House, pp. 25-43 (1981).
[9] Ki Hyeon Kim and Masahiro Yamaguchi, J. Appl. Phys. J. Appl. Phys. **99**, 08M902 (2006).
[10] C. Kittel, Phys. Rev. **73**(2), 155(1948).
[11] J. A. Osborn, Phys. Rev. **67**(11), 351 (1945).
[12] E. Van de Riet and F. Roozeboom, J. Appl. Phys. **81**(1), 350 (1997).
[13] Water Barry, IEEE Trans. Microwave & Tech, **MTT-34**(1), 80 (1986).